Dynamic interaction of bacterial cellulose synthase subunit D (BcsD) in type I bacterial cellulose synthase

Tatsuya Kondo[1], Yui Nakamura[2], Shingo Nojima[2], Min Yao[2*], Tomoya Imai[1*]

1 Research Institute for Sustainable Humanosphere (RISH), Kyoto University, Uji, Kyoto 611-0011, Japan.

2 Faculty of Advanced Life Science, Hokkaido University, N10W Kita-ku, Sapporo 060-0810, Japan.

*Corresponding authors:

Tomoya Imai, imai.tomoya.4c@kyoto-u.ac.jp; Research Institute for Sustainable Humanosphere, Kyoto University, Uji, Kyoto 611-0011, Japan.

Min Yao, yao@castor.sci.hokudai.ac.jp; Faculty of Advanced Life Science, Hokkaido University, N10W Kita-ku, Sapporo 060-0810, Japan.

Email: imai.tomoya.4c@kyoto-u.ac.jp

Author Contributions: T. I. and M. Y. conceptualization; T. K., T. I., and M. Y. methodology; T. K. formal analysis, T. K., N. Y., and S. N. investigation; T. I. resources; T. K. and T. I. data curation; T. K. and T. I. writing-original draft; T. K., M. Y., and T. I. writing-review and editing; T. K. and T. I. visualization; T. I. and M. Y. supervision; T. K., M. Y., and T. I. project administration; T. I. funding acquisition.

Competing Interest Statement: The authors declare that they have no conflicts of interest regarding the content of this article.

Classification: Biological Sciences

Keywords: cellulose, cellulose synthase, membrane enzyme, protein complex, polymer solid formation

This PDF file includes:

Main Text
Figures 1 to 7
Tables 1

Abstract

Cellulose is a promising biological material for supporting sustainable human life. This natural polymer is synthesized by cellulose synthase, a protein complex in the cell membrane. Cellulose synthase in bacteria is a hetero-subunit complex, and its subunit organization varies widely

depending on the species. In the type I bacterial cellulose synthase complex, the BcsD (bacterial cellulose synthase D) protein is believed to play an important role in producing cellulose with long slender fiber morphology and high crystallinity, given the phenotype of the bcsD-deficient mutant and the specific existence of the type I operon in bacterial species synthesizing crystalline cellulose microfibrils such as Acetobacter. In this study, we successfully established a heterogeneously expressed Bcs protein in Escherichia coli as an experimental model and conducted biochemical studies for the BcsD protein and the other three major subunits of bacterial cellulose synthase, BcsA, BcsB, and BcsC. It has been shown that the BcsD protein interacts with the functionally required minimal subunits of the BcsAB complex, as well as the BcsC protein. Furthermore, it was shown that BcsD interacts with the BcsAB complex in two modes: direct protein-protein interactions and indirect interactions through the product cellulose. The former and latter modes represent the basal and active states of the type I bacterial cellulose synthase, respectively. This dynamic behavior of the BcsD protein is important for the type I bacterial cellulose synthase complex to regulate the crystallization process of cellulose.

Significance Statement

Cellulose synthase is a membrane enzyme and its function is not only polymerization of glucose residues, but also bundling the polymerized glucan chains to form a slender crystalline fiber. This is a fascinating mechanism considering that long water-insoluble cellulose chains are actively assembled in aqueous solvent at room temperature. To clarify this mechanism as the protein function, this study analyzed bacterial cellulose synthase using protein purification experiments.

Main Text

Introduction

Cellulose is a natural polymer, whose molecular structure is composed of a homopolymer of glucose with a β1→4 linkage, which is very simple. However, cellulose molecules are insoluble in water, and the apparent elementary structure of cellulose is an aggregation of many cellulose molecules in long crystalline fibers. This structural feature of cellulose underlies its structure-sustaining property, which many cellulose-producing organisms rely on.

This polymer assembly is produced by the enzyme "cellulose synthase." In many known cases, *in vivo* cellulose synthase is a protein complex with several polypeptide subunits. The most important subunit in this complex is glycosyltransferase, which is called CesA. The first structural biological study of the CesA protein was reported in 2013 for cellulose synthase from the bacterium *Rhodobacter sphaeroides* (1, 2), which has stimulated many biochemical studies on cellulose synthase.

Given its simplicity, bacterial cellulose synthase (Bcs) has been a model in many studies on cellulose synthase. Particularly, Bcs from bacteria belonging to the genus *Acetobacter*, some of which are currently named as *Gluconacetobacter* or *Komagataeibacter* (the genus name "*Acetobacter*" is used for these bacteria in this study), has been used extensively in studies. Although it is now known that many other bacteria produce cellulose, the function and structure of cellulose appears to vary with species (3). For example, phosphoethanolamine cellulose has been reported in *Escherichia coli*, and this natural cellulose derivative is important for interacting with the host organism (4).

Among cellulose-synthesizing bacteria, *Acetobacter*, which has a gene cluster or operon categorized as type I (3), is characteristic of synthesizing highly crystalline cellulose microfibrils (5) as well as plant cellulose, a major natural source of cellulose. Previous studies have reported that the Bcs-complex in *Acetobacter* is composed of at least four subunits (6, 7) – BcsA (bacterial CesA, catalytic subunit), BcsB (auxiliary subunit having a carbohydrate-binding domain and flavodoxin domain), BcsC (secretion of a glucan chain through the outer membrane), and BcsD (crystallization subunit). In addition, endoglucanase CMCax (8, 9) (glycoside hydrolase family 8 (GH8)), unknown function protein Ccp (8, 10) (also named as BcsH (3)), and β-glucosidase bglAx (GH3) (11) are considered to be functionally involved in the complex. Given that the cooperation of these subunits produces highly crystalline cellulose microfibrils, the spatial organization of these subunits in the cell is important for understanding the cellulose biosynthesis mechanism as a protein function (12).

In these subunits, the BcsD protein is found specifically in bacterial species producing highly crystalline cellulose microfibrils such as *Acetobacter* and *Asaia* (3, 13, 14), which possess a type I Bcs-operon (3). The *bcsD*-deficient mutant of *Acetobacter* showed a reduction in cellulose production, as well as a lack of ability to synthesize crystalline cellulose microfibrils (6, 7, 15). Sunagawa *et al.* also demonstrated that BcsD interacts with Ccp (BcsH) in a pull-down assay (16). Given that the BcsD protein contains glucan chains inside its octamer structure (15), it has been proposed that BcsD is functionally located downstream of the BcsAB complex (the cellulose-polymerizing core of the Bcs-complex (1, 6, 17, 18)) (19, 20). Detailed information on how these functional units work together is key to understanding the mechanism by which cellulose synthase can bundle the synthesized glucan chains for spinning a long slender crystalline fiber at room temperature in an aqueous environment.

103 In this study, we analyzed protein-protein interactions in the type I Bcs-complex using the
104 recombinant BcsABCD protein with the *E. coli* expression system and clarified the interaction of
105 BcsD with BcsAB complex as well as BcsC protein. One of the advantages of using recombinant
106 proteins is that mutant proteins are easily available (21). Owing to this advantage, this study
107 sheds light on the interaction between BcsAB and BcsD and demonstrates that there are two
108 modes for this interaction: direct protein-protein interactions and indirect interactions through the
109 cellulose molecules. We hypothesized that such bimodal interactions between BcsAB and BcsD
110 proteins could be key to controlling cellulose synthesis dynamically *in vivo*.

111

112 Results

113 Production of endogenous *bcsA* gene-deficient *E. coli*

114 The expression of the *Acetobacter* Bcs complex in *E. coli* cells might lead to contamination by
115 endogenous *E. coli* Bcs (22).We then attempted to delete *bcsA* in the *E. coli* host, which encodes
116 the catalytic subunit of Bcs. The deletion of the *bcsA* gene in *E. coli* BL21, a strain expressing the
117 Bcs recombinant protein in this study, was performed using the Red/ET recombination system
118 (Gene Bridges GmdH, Germany), in which the *bcsA* gene was replaced by the FRT-PGK-gb2-
119 neo-FRT cassette with homology arms of the *bcsA*-flanking region using homologous
120 recombination (Fig. 1A). This genetically modified BL21 (BL21-GM) strain was confirmed by
121 colony direct polymerase chain reaction (PCR) to contain the neomycin-resistance gene cassette
122 (FRT-PGK-gb2-neo-FRT cassette) (Fig. 1B). When amplified with primer #2 (antibiotic gene
123 cassette-specific) and #3 (*E. coli*-specific), a band of approximately 1,500 bp was found in BL21-
124 GM, while no specific product band was found in wild-type BL21, indicating the insertion of the
125 neomycin-resistance gene cassette specifically in BL21-GM. However, when amplified with
126 primers #1 and #3 (either *E. coli*-specific), wild-type BL21 and BL21-GM produced a band
127 corresponding to the *bcsA* gene (2,818 bp) and the inserted gene cassette (1,731 bp), respectively.
128 These results confirmed the successful deletion of the *bcsA* gene of BL21 in "BL21-GM."

129 Next, we measured the *in vivo* cellulose synthesis activity of the prepared BL21-GM (Fig. 1C)
130 by partially using our previous method (18): diguanylate cyclase (DGC) fused to thioredoxin
131 ($_{Trx}$DGC) was expressed in BL21 and BL21-GM to synthesize c-di-GMP to activate endogeneous
132 bacterial cellulose synthase. The amounts of cellulose synthesized were approximately 2.3 and
133 0.7 μg/mL of culture in BL21 and BL21-GM, respectively. Although weak cellulose-synthesizing
134 activity was observed, we used BL21-GM as a suitable host to express the Bcs subunits with
135 minimal impact on the endogenous Bcs-complex of *E. coli*.

136

137 Characterization of BsCel5A

138 Cellulase is an important tool used in this study to scrutinize the role of cellulose molecules in
139 the subunit-subunit interaction of the Bcs-complex. In this study, we used a bacterial endo-β-1,4-
140 glucanase from *Bacillus subtilis* (BsCel5A), whose structure has been previously reported (23).
141 The full length (FL) of this cellulase is a two-domain protein, in which the catalytic domain of
142 GH5 is linked to the carbohydrate binding module of family 3 (CBM3). In this study, the catalytic
143 domain alone (CD) was also used to maximize access to the soluble substrate. FL and CD of
144 BsCel5A were expressed as glutathione-*S*-transferase (GST)-fused proteins and purified with
145 glutathione affinity resin, as confirmed by SDS-PAGE (Fig. S1A, left panel); (Fig. S1A, left

panel, white arrow). Activity-deficient mutant of E169Q/E257Q in FL (BsCel5A_FLm) and CD (BsCel5A_CDm) was also used for a negative control protein in the cellulase treatment experiment.

The binding activity of the purified BsCel5A to phosphoric acid-swollen cellulose (PASC) was surveyed to confirm correct folding of the expressed proteins. The results showed that all the BsCel5A proteins used in this study retained their binding activity to PASC (Fig. S1A, right panel), indicating that all of them were properly folded despite sequence modification. The enzymatic activity of BsCel5A was surveyed to determine whether this cellulase could function at low temperature and neutral pH, which is required for analyzing the Bcs-complex. Both BsCel5A_FL and BsCel5A_CD hydrolyzed barley β-glucan, carboxyl methyl cellulose (CMC), and PASC at 4°C and pH 7.5 (Fig. S1B). For Avicel, full-length BsCel5A showed higher activity than the others, stressing the function of CBM to bind solid cellulose.

Substrate specificity of BsCel5A was investigated using cello-oligosaccharides with various degrees of polymerization (DP). BsCel5A hydrolyzed cellotetraose, cellopentaose, and cellohexaose but not cellobiose or cellotriose (Fig. S1C). The final reaction products of BsCel5A for substrates longer than triose were cellobiose and cellotriose, and the smallest substrate was cellotetraose (Fig. S1D).

Summarizing these, both BsCel5A_FL and BsCel5A_CD were able to hydrolyze cellulose of low crystallinity at 4°C and pH 7.5, and cellulose molecules with DP higher than 3 were the substrates. This information was considered when interpreting the data.

In vivo cellulose synthase activity of recombinant Bcs-complex

This study analyzed heterogeneously expressed Bcs proteins in *E. coli* as an experimental model. We then checked if these heterogeneously expressed proteins were functional by using CESEC (cellulose-synthesizing *E. coli*), a platform for estimating the cellulose-synthesizing activity with the co-expression of diguanylate cyclase (DGC) (18). All the Bcs-complexes expressed in DGC-expressing BL21-GM synthesized a significant amount of cellulose (Fig. 2A), indicating that each of the Bcs-complexes expressed in this study are functional, regardless of whether BcsD is tagged. In addition, neither BcsAB nor the BcsABCD complex with the activity-deficient mutant of the catalytic subunit BcsA (D333N or W373A) showed cellulose-synthesizing activity, consistent with our previous study (21). These results support the idea that the Bcs proteins expressed in this study reflect the state in function and are suitable for an experimental model.

Despite the lower cellulose production shown in Fig. 2A, we decided to express Bcs proteins without co-expression of DGC for subsequent purification because higher expression levels of Bcs proteins were detected by western blotting (WB), as shown in Fig. 2B. Given that the cellulose quantification in this study used strong acid treatment with acetic acid and nitric acid, we think that highly crystalline cellulose was majorly considered in the data presented in Fig. 2A. Then it cannot be ruled out that the Bcs-complex expressed in *E. coli* without DGC expression synthesizes cellulose.

The complex formation of BcsAB, BcsC, and BcsD

188 Given that BcsD holds the glucan chains in its channel (15), it is functionally located
189 downstream of the BcsAB complex, the core of cellulose molecule synthesis, indicating that
190 BcsD operates in the periplasmic space to assemble cellulose molecules extruded from the
191 BcsAB complex. Furthermore, the BcsC protein has a β-barrel porin-like structure at its C-
192 terminus and is supposed to secrete cellulose through the outer membrane (24). The results from
193 several studies suggest that BcsAB, BscC, and BcsD work together in a coordinated manner to
194 spin bacterial cellulose. We tried to co-express BcsABCD to purify the whole Bcs-complex using
195 a hexa-histidine tag attached to the C-terminus of BcsD ($BcsD_{H6}$), as the tag at the C-terminus
196 does not disturb cellulose-synthesizing activity (16). After the optimization of the conditions (Fig.
197 S2), all four subunits were successfully purified together by immobilized metal affinity
198 chromatography (IMAC) (Fig. 3). This is the first successful purification of the BcsABCD
199 complex ever reported. However, BcsC was found to be mostly insoluble in detergent (*n*-dodecyl-
200 β-D-maltoside, DDM, in this study) and tended to degrade or aggregate during the purification
201 process (Fig. 3A, BcsC antibody strip). We did not decipher BcsC behavior in this Bcs-complex
202 purification experiment.

203

204 **Analysis of the interaction between BcsAB and BcsD by cellulase treatment**

205 As described above, co-expression of $BcsABCD_{H6}$ in *E. coli* allowed the BcsABD-complex to
206 be purified. Given that $BcsABCD_{H6}$ expressed in *E. coli* is functional as shown in Fig. 2A, we
207 speculated that a glucan chain may link BcsAB and BcsD during this purification. This
208 hypothesis was tested by checking whether the digestion of cellulose resulted in the dissociation
209 of BcsAB from $BcsD_{H6}$ during IMAC purification. BsCel5A cellulase was applied to
210 $BcsABCD_{H6}$ bound to IMAC resin prior to washing and elution. The amounts of BcsA, BcsB,
211 and BcsD proteins in the eluate were measured by semi-quantitative WB (Fig. 4A); the reliability
212 of quantification in our WB was confirmed, as shown in Fig. S3. The signal intensities of BcsA
213 and BcsB were normalized to that of BcsD in the eluate for comparison between samples.
214 Notably, the amounts of BcsA and BcsB bound to BcsD were decreased by BsCel5A treatment
215 (Fig. 4B), indicating that the BcsAB complex was detached from BcsD by cellulose digestion.
216 This trend was clearer when BsCel5A_CD was used as cellulase.

217 To rule out the possibility that the observed detachment of BcsAB was due to non-specific
218 interaction of the added BsCel5A protein, the activity-deficient mutant of BsCel5A
219 (E169Q/E257Q) was applied to $BcsABCD_{H6}$ bound to the metal affinity resin (Fig. 4, C and D).
220 As a result of purification, no decrease in the signal intensity of BcsA and BcsB was observed in
221 the eluate, indicating that cellulose hydrolysis actually caused detachment of BcsAB from BcsD
222 during purification. In summary, the BcsAB complex indirectly interacts with BcsD through the
223 glucan chain.

224 Although cellulase treatment allowed the BcsAB complex to be detached from BcsD during
225 purification, as demonstrated above, a substantial portion of the BcsA and BcsB proteins
226 remained with BcsD in this purification process (Fig. 4B). We supposed that a direct interaction
227 between BcsAB and BcsD is also found in addition to the indirect interaction. To test this
228 hypothesis, we attempted to purify the activity-deficient mutants of $BcsABCD_{H6}$,
229 $BcsA^{D333N}BCD_{H6}$, and $BcsA^{W373A}BCD_{H6}$, neither of which synthesize cellulose, as shown in Fig.
230 2A. As a result, these mutants allowed BcsA and BcsB to be purified together with BcsD and the
231 wild type (Fig. 5A and B). Notably, cellulase treatment did not reduce the amount of BcsAB
232 purified together with BcsD for either $BcsA^{D333N}BCD_{H6}$ or $BcsA^{W373A}BCD_{H6}$ (Fig. 5C, 5D, and

5E). These results support the existence of a direct interaction between BcsAB and BcsD when cellulose is not synthesized. Compiling these cellulase treatment experiments, it was demonstrated that there are two modes of interaction between BcsAB and BcsD: direct and indirect modes through cellulose molecules.

Quaternary structure of the Bcs-complex

Despite the demonstration of two modes for the interaction between BcsAB and BcsD, the quaternary structure of the entire Bcs-complex remains to be elucidated. We then performed pull-down assays to further explore the subunit-subunit interactions in the BcsABCD complex by fully utilizing recombinant Bcs proteins. The assay was designed based on the results from previous studies (Fig. 6A): (i) BcsAB forms a complex in the inner membrane (1), (ii) BcsC is an outer membrane protein (24, 25), (iii) BcsD protein is located in the periplasmic space (15, 20), and (iv) BcsD interacts with the BcsAB complex (this study).

First, the interaction between BcsAB and BcsD, which has been demonstrated above, was tested by pull-down with a bait of Streptag(II)-fused BcsD ($BcsD_{StrepII}$) and a prey of crude BcsAB without tags (DDM-solubilized cell membrane of *E. coli* expressing BcsAB). As expected, BcsAB bound to $BcsD_{StrepII}$ (Fig. 6B). The pull-down assay yielded a result consistent with our purification experiment of the BcsABD-complex and supported our hypothesis for the interaction between BcsAB and BcsD.

Given the successful pull-down assay with BcsAB and $BcsD_{StrepII}$, we next performed a pull-down assay to survey the BcsC-involved interaction in the complex (see Fig. 6A). For this purpose, TPR tetratricopeptide-repeat (TPR) domain of the BcsC protein (BcsC_TPR) was used based on two assumptions: (i) the role of the TPR domain is protein-protein interaction (26), and (ii) the full-length BcsC protein is unstable, as shown in our purification. Pull-down by $BcsD_{StrepII}$ trapped $_{H6}BcsC_TPR_{H6}$, which has hexa-histidine tags at both the N- and C-termini of BcsC_TPR, in a dose-dependent manner (Fig. 6C), clearly showing that these two proteins interact with each other. Furthermore, pull-down by the purified $_{H6}BcsC_TPR_{H6}$ (bait) with the crude BcsAB (prey) also supported their interaction with each other (Fig. 6D), although it appeared less striking than the case with $_{H6}BcsC_TPR_{H6}$ and $BcsD_{StrepII}$ (Fig. 6C).

Finally, we performed a pull-down assay using all subunits in the complex: crude BcsAB, purified $_{H6}BcsC_TPR_{H6}$, and purified $BcsD_{StrepII}$ (Fig. 6E). Streptactin beads trapped BcsA, BcsB, and $_{H6}BcsC_TPR_{H6}$ together with $BcsD_{StrepII}$, although BcsA was only faintly detected by WB. It is then summarized that the BcsD protein can simultaneously interact with BcsA, BcsB, and the TPR region of BcsC.

Discussion

Bacterial cellulose synthase is a heterosubunit complex. Primary evidence for this hypothesis is the existence of gene clusters or operons encoding cellulose synthase-related genes (3, 6, 7, 11). However, this hypothetical model has not been tested intensively, owing to the lack of studies on the protein. Two recent reports have addressed this question. Sunagawa et al. demonstrated an interaction between BcsD and BcsH (Ccp) proteins using a pull-down assay (16). Another prominent study was the X-ray crystallographic analysis of the BcsAB protein complex by

Morgan et al., which clarified that the BcsA and BcsB proteins closely interact with each other to polymerize and translocate the glucan chain from the cytosol to the extracellular side (1), as confirmed also in *E.coli* (27). In this study, we analyzed the type I Bcs complex and demonstrated that the BcsD protein interacted with the BcsAB complex (Fig. 3, 4, 5, and Fig. 6B) and the TPR domain of BcsC (Fig. 6C). Furthermore, it was shown that BcsC_TPR interacted with the BcsAB complex, although the result was not as clear as the interaction between BcsC_TPR and BcsD (Fig. 6D). Finally, a pull-down assay using $BcsD_{StrepII}$ with a mixture of crude BcsAB and purified $_{H6}$BcsC_TPR$_{H6}$ indicated that BcsD binds to both BcsAB and BcsC_TPR simultaneously, suggesting that these four subunits interact with each other (Fig. 6E). Our study, together with previous studies, experimentally demonstrated that the subunits of BcsA, BcsB, BcsC, BcsD, and BcsH are included in the type I Bcs-complex.

Interestingly, this study showed that the interaction of BcsD with BcsAB has two modes: direct and indirect interactions through the polymerized glucan chain (Fig. 4). Direct interaction between the BcsAB complex and BcsD protein was observed for both wild type and catalytically deficient mutant cellulose synthase, whereas the interaction via cellulose was observed only for the wild type (Fig. 5). We then propose a two-state model for the type I Bcs complex: basal and active states, which are represented by the direct interaction (Fig. 7, left) and indirect interaction modes (Fig. 7, right), respectively.

BcsD protein in this basal state is statically fixed on the BcsAB complex for lying in wait for a glucan chain synthesized by the BcsAB complex. Once cellulose synthesis is initiated, the synthesized glucan chain is guided into the octameric ring of BcsD to crystallize cellulose molecules, as proposed previously (7, 15, 16, 20, 28), which is a shift from the resting state to the active state of the complex. In the active state (Fig. 7, right), the BcsD protein is detached from the BcsAB complex but tethered to BcsAB by the glucan chain extruded from BcsAB. Considering the substrate specificity of BsCel5A (Fig. S1), BcsD can be physically separated from BcsB by a glucan chain with a length of four or more glucose residues (Fig. 7).

In this two-state model, the active state of the Bcs complex allows BcsD to be launched toward the outer membrane, while BcsD in the basal state may be fixed statically on BcsB. The TPR domain of the BcsC protein may control diffusible BcsD in the active state in the periplasmic space by gentle but significant interactions. Given that the C-terminal domain of BcsC is an outer membrane β-barrel channel (Fig. S4) (24), the TPR domain of BcsC may escort BcsD carrying glucan chains toward the outer membrane channel in BcsC to spin the glucan chains to the extracellular side. The following questions about this model will be whether (i) BcsD protein could dock to the outer membrane channel part of the BcsC protein and (ii) the interaction between BcsC and BcsD could be state-dependent. These questions will be addressed in future studies to enhance our understanding of the Bcs-complex function.

Our study demonstrated the intermolecular interactions of subunits in the BcsABCD complex to update our knowledge of the quaternary structure of the type I Bcs complex. Experiments in this study were performed using recombinant proteins heterogeneously expressed in *E. coli*; thus, further studies will be necessary to test the hypothesis proposed in this study, the two modes for BcsAB-BcsD interaction: the basal and the active state. Nonetheless, the data obtained in this study were intensively tested using mutagenesis experiments of proteins, and they were consistent with each other. We believe that our hypothesis in this study is sufficiently reliable, at least for starting further discussion about the mechanism of Bcs with regard to protein function. In this model, BcsD is not statically fixed in the Bcs-complex but dynamically interacts with the other subunits in the complex (Fig. 7). Such a dynamic behavior may be involved in the crystallization

321 function of cellulose molecules, as well as twisting in bacterial cellulose microfibrils, as reported
322 previously (16). The putative state control with BcsD, as shown in Fig. 7, is the regulation of the
323 quaternary structure of bacterial cellulose synthase. Next, we need to further study the original
324 *Acetobacter* cells and observe the whole Bcs-complex at higher resolution with cryo-EM under
325 controlled two-state conditions.

326
327
328 **Materials and Methods**
329
330 **Chemicals**

331 All chemicals used in this study were purchased from FUJIFILM Wako Pure Chemicals Co.
332 Ltd. (Osaka, Japan), Nacalai Tesque Co. Ltd. (Kyoto, Japan), and Sigma-Aldrich Inc. (MO,
333 USA), unless otherwise indicated.

334

335 **Cloning**

336 Bcs genes (*bcsA*, *bcsB*, *bcsC*, and *bcsD*) were prepared from genomic DNA extracted from
337 cultured cells of *Komagataeibacter sucrofermentans* JCM9730, which was provided by the
338 RIKEN Bio Resource Center (Tsukuba, Japan) and known by the strain name BPR2001 (29, 30).
339 The endo-β1,4-glucanase gene from *Bacillus subtilis* strain 168 (*bscel5A*) (23) was prepared from
340 the genomic DNA provided by the American Type Culture Collection (ATCC23857D). The dgc
341 gene (*dgc*) was identical to that used in our previous study (18): tDGC and DGC from
342 *Thermotoga maritima* MSB8 with a point mutation of R158A and truncation of the N-terminal 81
343 amino acid residues from V1 to V81 (31). The gene for green fluorescent protein UV (GFPuv)
344 (32) was prepared from the pGFPuv plasmid purchased from Takara Bio, Co. Ltd. (Shiga, Japan).

345 The cloning of these genes was performed by PCR using PrimeStarGXL (Takara Bio Co. Ltd.).
346 Site-directed mutagenesis was performed by QuikChange II (Agilent Inc., CA, USA) or the
347 equivalent PCR-based method. The sequence of the PCR-amplified DNA was checked by the
348 dye-terminator method in a subcloning vector (pGEM-T easy (Promega Inc., WI, USA) or pTAC-
349 2 (BioDynamics Laboratory Co. Ltd., Tokyo, Japan)), or final expression vector, which was
350 performed at either of the Uji DNA-sequencing core (Kyoto University Research Administration
351 Office) with an ABI Prism 310 Genetic Analyzer (Applied Biosystems Inc., MA, USA), or
352 Eurofins Genomics Inc. (Tokyo, Japan).

353

354 **Construction of the expression vectors**

355 The protein expression vectors used in this study are summarized in Table 1. Expression
356 vectors for BcsAB (BcsWTB, $BcsA^{D333N}B$, and $BcsA^{W373A}B$) were identical to those used in
357 previous studies (18, 21). The *bcsAB* gene in the operon form was inserted between the EcoRI
358 and KpnI sites in pQE-80L (Qiagen, Hilden, Germany), and the upstream of the start codon was
359 the original ribosomal binding site of *K. sucrofermentans* JCM9730.

360 Expression vectors for BcsABCD (BcsABCD, $BcsABC_{H6}D$, $BcsABCD_{H6}$, $BcsA^{D333N}BCD_{H6}$,
361 $BcsA^{W373A}BCD_{H6}$, and $BcsABCD_{GFPuvH6}$) proteins were constructed from the vectors for BcsAB
362 by inserting the *bcsABCD* gene in the operon form between the EcoRI and HindIII sites in pQE-

363 80L. The ribosomal binding site in these BcsABCD expression vectors is exactly the same as that
364 in the expression vectors of BcsAB, one of *K. sucrofermentans* JCM9730. DNA encoding the tag
365 (hexa-histidine or GFPuv) was added to *bcsD* during the PCR-amplification amplification.

366 The expression vectors for the TPR region of BcsC (BcsC_TPR: C18-G848) and BcsD were
367 prepared for the pull-down assay. DNA encoding hexa-histidine tag was added to the 3′-end of
368 the gene for BcsC_TPR during PCR amplification and inserted into the NdeI and XhoI sites in
369 pET-28b (Merck Corp.., Darmstadt, Germany) to express BcsC_TPR protein with dual hexa-
370 histidine tag at both N- and C- terminal – $_{H6}$BcsC_TPR$_{H6}$. DNA encoding Streptag (II) was added
371 to the 3′-end of the gene for BcsD and inserted between the NcoI and HindIII sites in pET28b to
372 express BcsD with C-terminal Streptag(II)–BcsD$_{StrepII}$.

373 The gene for tDGC was inserted between the NdeI and HindIII sites in pBAD33et32, a
374 customized plasmid DNA in this study, to express the thioredoxin-fused tDGC protein to count
375 the cellulose-synthesizing activity of the recombinant BcsAB and BcsABCD complex in our
376 previous studies (18, 21). The detailed procedure for preparing pBAD33et32 is described in
377 Supplementary Information. Thioredoxin gene (*trx*) in pBAD33et32 was copied from pET32a
378 (Merck Corp.) to replace the His-patch thioredoxin used in our previous study (18), which was
379 derived from pBAD202-TOPO (Invitrogen Inc., MA, USA).

380 For the bacterial endoglucanase gene *bscel5A*, the putative signal peptide sequence (M1–A28)
381 was removed from the full-length construct. Full-length (A29–N499) and catalytic domain (A29–
382 T332) genes were inserted between BamHI and XhoI sites in pGEX4T-3 (Cytiva Inc., MA, USA)
383 to express the N-terminal GST-fused endoglucanase BsCel5A.

384

385 **Deletion of *bcsA* gene from *Escherichia coli* BL21**

386 In this study, we used genetically modified *E. coli* BL21 to express Bcs proteins, which lack
387 the whole *bcsA* gene (Fig. 1A). This gene manipulation was performed using the Red/ET
388 recombination system (Gene Bridges GmbH, Heidelberg, Germany), according to the
389 manufacturer's specifications. The detailed procedure is described in Supplementary Information.

390 Briefly, *E. coli* BL21 strain (purchased from New England Labs Inc., MA, USA) was
391 transformed with the pRedET plasmid carrying the genes for DNA-recombination proteins and
392 selected by tetracycline resistance. The second transformation was followed by introducing linear
393 DNA of neomycin-resistant gene flanked by the homology arm sequences corresponding to the
394 upstream and downstream of *bcsA* gene (CP010816.1); the recombinant proteins were expressed
395 with arabinose-induction for disrupting *bcsA* gene, and subsequently the pRedET plasmid was
396 expelled out of the cell by culturing at 37°C. Finally, the *bcsA-disrupted* BL21 transformant was
397 selected for kanamycin resistance and tetracycline sensitivity. Gene modification was confirmed
398 by direct PCR (Fig. 1B). We named this genetically modified *E. coli* BL21 strain as BL21-GM.
399 Chemically competent cells of BL21-GM were then prepared by treating the cultured cells in a
400 rubidium-based buffer according to the protocol on the website of the Center for Molecular
401 Biology and Genetics at Mie University (https://www.gene.mie-
402 u.ac.jp/Protocol/Original/Transform-Comp-Cell-Freeze.html, in Japanese) (33).

403

404 ***In vivo* cellulose synthase activity**

405 The endogenous cellulose-synthesizing activity of *E. coli* and cellulose-synthesizing activity of
406 the heterogeneously expressed Bcs-complex in *E. coli* was estimated by expressing DGC protein
407 to activate bacterial cellulose synthase in the cell by the produced c-di-GMP (18). In this study,
408 the pBAD33et32-tDGC plasmid was used to express the DGC. The obtained *E. coli*
409 transformants were pre-cultured in LB medium including the proper antibiotics at 37°C
410 overnight, and then 0.1 mL of the pre-culture was inoculated into 10 mL of ZYP-5052 medium
411 with 50 μg/mL chloramphenicol (100 μg/mL ampicillin when expressing Bcs-complex) and
412 0.001% L-arabinose. Cells were grown at 20°C in an orbital shaker at 180 rpm for 24 h and the
413 cultured cells were collected by centrifugation at 2,000 × *g* for 20 min. The amount of cellulose in
414 the pellet was quantified using the anthrone-sulfuric acid method (34) as described below.

415 Two milliliters of AN-reagent (a mixture of glacial acetic acid and nitric acid with volumetric
416 ratio of 8:1) were added to the pellet and then heated at 105°C for 30 min. The remaining
417 cellulose pellets were washed with 10 mL of water once by centrifugation at 2,000 × *g* for 10
418 min, and then 1 mL of 72% (v/v) H_2SO_4 was added to the pellets and incubated for 1 h at room
419 temperature. The solution (0.1 mL) was mixed with water (0.4 mL), and then, 1 mL of fresh
420 anthrone reagent (0.2% w/v anthrone in concentrated H_2SO_4) was added and mixed. The solution
421 was heated to 90°C for 15 min and allowed to stand until it reached room temperature
422 (approximately 15 min). The absorbance of the solution was measured at both 625 and 700 nm,
423 and the absorbance at 625 nm, from which the absorbance at 700 nm was subtracted, was used for
424 quantification for better reproducibility. Calibration was performed with phosphoric acid-swollen
425 cellulose (PASC) prepared using a previously reported protocol (35).

426

427 **Purification and characterization of BsCel5A**

428 Expression of GST-fused BsCel5A endoglucanase was performed in *E. coli* BL21 (not GM
429 strain): all the four constructs ((BsCel5A_FL, BsCel5A_CD, BsCel5A_FL^m, and BsCel5A_CD^m)
430 were expressed and purified in the same manner.

431 The transformant of BL21 with pGEX-BsCel5A were inoculated in 10 mL LB containing 100
432 μg/mL ampicillin in a 100 mL flask and grown at 37°C with orbital shaking at 220 rpm overnight.
433 The cells were harvested by centrifugation at 3,000 × *g* for 20 min, suspended in 1 L of LB
434 containing 100 μg/mL ampicillin in a 5 L baffle flask, and cultured at 37°C until OD_{600} reached
435 0.6. The culture medium was cooled in ice water for 10 min, and then IPTG was added to 0.1 mM
436 and incubated at 20°C for 20 h at 160 rpm with shaking.

437 The cells were then collected at 3,000 × *g* for 20 min, washed with 40 mL of 1 × phosphate-
438 buffered saline (PBS), suspended in 40 mL of 1 × PBS containing 1 mM phenylmethylsulfonyl
439 fluoride (PMSF), and sonicated on ice for ~5 min (exposure: 10 s, rest: 50 s; until slightly
440 translucent). The cell lysate clarified by 20,000 × *g* for 30 min at 2°C was applied to 5 mL of
441 Glutathione Sepharose 4B (Cytiva Inc,), washed with 20 mL of 1 × PBS, and eluted with 5 c.v. of
442 0.1 M Tris-HCl pH 8.0, 0.5 M NaCl, 20 mM reduced-glutathione. The eluted fraction was buffer
443 exchanged with 1 × PBS using Vivaspin 6 (MWCO 10 kDa; Sartorius AG, Germany).

444 To remove the GST tag fused to the N-terminus, 100 units of thrombin (Merck Corp.) was
445 added to 10 mg of $_{GST}$BsCel5A and incubated at 20°C for two days. Thrombin was then removed
446 by adding 1 mL of Benzamidine Sepharose 6 B (Cytiva Inc.), and the cleaved GST was removed
447 by adding 5 mL of Glutathione Sepharose 4 B. A solution of PMSF was added to the obtained

448 BsCel5A protein at a final concentration of 1 mM to inactivate a small amount of residual
449 thrombin.

450 The recombinant BsCel5A proteins purified were characterized with regard to the following
451 points: (i) binding activity to cellulose, (ii) glycoside hydrolase activity, and (iii) substrate
452 specificity. The detailed experimental procedure is described in Supplementary Information.

453

454 **Purification of BcsABCD complex**

455 All the protein purification experiments in this study were performed at low temperature
456 (~4°C). The composition of the protease inhibitor mix (PI) used for protein purification was as
457 follows: 0.1 mM PMSF, 1 mM benzamidine-HCl, 5 μM bestatin, 10 μM leupeptin, 1 μM
458 pepstatin A.

459 The transformant of *E. coli* BL21-GM with pQE-BcsABCD$_{H6}$ was inoculated in 10 mL of LB
460 containing 100 μg/mL ampicillin in a 100 mL flask and grown at 37°C with shaking at 220 rpm
461 overnight. The cells were harvested by centrifugation at 3,000 × *g* for 20 min, resuspended in 1 L
462 of ZYP-5052 containing 100 μg/mL ampicillin and 0.0005% (v/v) antifoam SI (Fujifim Wako
463 Chemicals Co. Ltd., Japan) in a 5 L baffle flask, and incubated at 20°C for 22 h with an orbital
464 shaker at 100 rpm. The cultured cells were collected at 3,000 × *g* for 20 min and suspended in 50
465 mL of buffer A (20 mM sodium phosphate buffer (pH 7.5), 300 mM NaCl, 8% glycerol, 5 mM
466 $MgCl_2$, 5 mM cellobiose) with PI, prior to cell lysis by two passes of high-pressure homogenizer
467 (French Press, Thermo Fisher Scientific Inc., MA, USA) at a pressure of 15,000 psi. The lysate
468 clarified by centrifugation at 5,000 × *g* for 10 min and ultracentrifugation at 150,000 × *g* for 30
469 min at 2°C. The obtained cell membranes were resuspended in buffer A with PI and NaCl
470 concentrations increased to 1 M and were ultracentrifuged again under the same conditions.
471 Finally, the cell membrane was suspended in buffer A with PI to approximately 10 mg/mL
472 (estimated by the DC protein assay, Bio-Rad Inc., CA, USA). The collected cell membrane was
473 stored at -80°C until use in experiments.

474 Ten milliliters of the cell membrane suspension were mixed with *n*-dodecyl-β-D-
475 maltopyranoside (DDM) at a final concentration of 0.5% (w/v) and shaken gently for 1 h at 4°C
476 for solubilizing Bcs-complex. Supernatant of the following ultracentrifugation at 150,000 × *g* for
477 30 min at 2°C was collected as solubilized fraction, and imidazole stock solution (2 M, pH 8.0)
478 was added to achieve a final concentration of 10 mM, prior to loading to 0.4 mL a His-Select
479 Cobalt Affinity Gel (Sigma-Aldrich Inc.), which was equilibrated with 4 mL of wash buffer (20
480 mM imidazole and 0.025% (w/v) DDM in buffer A) in advance. After loading the solubilized
481 protein onto the affinity resin in a plastic open column, the resin in the column was washed with 3
482 mL of wash buffer and finally eluted with elution buffer (200 mM imidazole and 0.025% (w/v)
483 DDM in buffer A).

484

485 **Cellulase treatment of Bcs-complex**

486 Cellulase treatment of BcsABCD$_{H6}$ was performed using a cobalt affinity gel. The same
487 procedure was followed for the binding step of BcsABCD$_{H6}$ on the affinity gel. After all the
488 solubilized fraction passed through the column, 0.8 mL of 1.5 μM BsCel5A solution in wash
489 buffer (20 mM imidazole and 0.025% (w/v) DDM in buffer A) was loaded to the column. The

490 column exit was plugged when most of the cellulase solution passed, and then the gel was
491 incubated at 10°C for 3 h with the remaining cellulase solution. After unplugging, the affinity gel
492 in the column was washed with 2 mL of wash buffer and eluted with elution buffer (200 mM
493 imidazole and 0.025% (w/v) DDM in buffer A).

494

495 **Protein preparation for pull-down assay: BcsC_TPR, BcsD, and crude BcsAB**

496 The pull-down assay in this study used purified BcsC_TPR, purified BcsD, and crude BcsAB
497 proteins, each of which was prepared as described below.

498 The transformant of *E. coli* BL21(DE3) with pET-$_{H6}$BcsC_TPR$_{H6}$ was inoculated in 10 mL of
499 LB containing 50 µg/mL kanamycin in a 100 mL flask and grown at 37°C with shaking at 220
500 rpm overnight. The cells were harvested by centrifugation at 3,000 × *g* for 20 min, and
501 resuspended in 1 L of ZYP-5052 (36) containing 200 µg/mL kanamycin and 0.0005%(v/v)
502 antifoam SI in a 5 L baffle flask, and incubated at 20°C for 24 h in a shaking incubator at 100
503 rpm. The cultured cells were collected at 3,000 × *g* for 20 min, and washed with 40 mL of 1 ×
504 PBS prior to resuspension in 100 mL of 10 mM imidazole in buffer B (20 mM sodium phosphate
505 buffer (pH 7.5), 500 mM NaCl, 8% glycerol) with PI, and sonicated on ice for ~5 min (exposure:
506 10 s, rest: 50 s; until slightly translucent). The cell lysate was clarified by centrifugation at 40,000
507 × *g* for 30 min at 2°C and applied to 4 mL a His-Select Cobalt Affinity Gel (Sigma-Aldrich Inc.),
508 followed by washing with 10 mM imidazole in buffer B, and eluted 250 mM imidazole in buffer
509 B. Finally, the buffer of eluted fraction including $_{H6}$BcsC_TPR$_{H6}$ protein was replaced with buffer
510 B using PD-10 desalting column (Cytiva Inc.).

511 The BcsD protein was expressed in *E. coli* BL21(DE3) with pET-BcsD$_{StrepII}$. The transformant
512 was inoculated in 10 mL of LB containing 50 µg/mL kanamycin in a 100 mL flask and grown at
513 37°C with shaking at 220 rpm overnight. The cells were harvested by centrifugation at 3,000 × *g*,
514 20 min, resuspended in 1 L of LB containing 50 µg/mL kanamycin in a 5 L baffle flask and
515 cultured at 37°C until OD_{600} was ~0.6. The culture medium was cooled in ice water for 30 min,
516 and IPTG (0.5 mM) was added and incubated at 25°C for 20 h at 120 rpm. Cells were collected at
517 3,000 × *g* for 20 min, suspended in 30 mL of buffer C (20 mM Tris-HCl (pH 7.5), 150 mM NaCl,
518 and 1 mM EDTA) with PI, and sonicated on ice for ~10 min (exposure: 10 s, rest: 50 s; until
519 slightly translucent). The cell lysate was centrifuged at 20,000 × *g* for 30 min at 2°C, applied to 2
520 mL of Streptactin Sepharose HP (Cytiva Inc.), washed with 20 mL of buffer C, and eluted with 4
521 mM *d*-desthiobiotin in buffer C. Finally, buffer of eluted fraction was replaced by buffer C using
522 Amicon Ultra-4 MWCO 50 kDa (Merck Corp.).

523 The crude protein of BcsAB was prepared using the transformant *E. coli* BL21-GM with pQE
524 carrying the *bcsAB* gene. The procedure to isolate the cell membrane, from culture to
525 ultracentrifugation, was same as in the case of BcsABCD$_{H6}$ as described previously, except for
526 the buffer to suspend the cells and cell membrane: buffer D (20 mM sodium phosphate buffer (pH
527 7.5), 100 mM NaCl, 8% glycerol, 5 mM $MgCl_2$, and 5 mM cellobiose) with PI was used. The
528 obtained cell membrane was suspended in buffer D with PI at approximately 10 mg/mL
529 (estimated by the DC protein assay, Bio-Rad Inc.). Finally, crude BcsAB protein was prepared by
530 solubilizing 7 mL of the cell membrane fraction with 0.5% (w/v) DDM for 1 h and centrifugation
531 at 150,000 ×*g* for 30 min at 2°C.

532

533 **Pull-down assays**

534 For the pull-down by $BcsD_{StrepII}$ with the crude BcsAB, purified $BcsD_{StrepII}$ (0.2 mg) was added
535 to 7 mL of crude BcsAB, incubated for 3 h at 4 °C, and then loaded to 0.1 mL of Streptactin
536 Sepharose HP. The resin was washed with 1 mL of 0.025% (w/v) DDM in buffer D, and finally
537 the bound protein was eluted with 4 mM desthiobiotin in buffer D with 0.025% (w/v) DDM.

538 For the pull-down assay, $BcsD_{StrepII}$ with $_{H6}BcsC_TPR_{H6}$, $BcsD_{StrepII}$ (0.1 mg) were incubated
539 with $_{H6}BcsC_TPR_{H6}$ (0, 0.1, 0.3, 0.5 mg) in 3 mL of buffer D (–/–) (buffer D without $MgCl_2$ and
540 cellobiose) for 3 h at 4 °C, and then loaded to 0.1 mL of Streptactin sepharose HP. After washing
541 with buffer D (–/–), the bound protein was eluted with 1 mL 4 mM *d*-desthiobiotin in buffer D (–
542 /–).

543 For the pull-down assay by $_{H6}BcsC_TPR_{H6}$ with BcsAB, purified $_{H6}BcsC_TPR_{H6}$ (0.2 mg) was
544 mixed with crude BcsAB (7 mL), and further NaCl stock solution was added to set 500 mM NaCl
545 in the final solution. After incubation for 1 h at 4 °C, the sample was loaded to 0.2 mL a His-
546 Select Cobalt Affinity Gel and washed with 2 mL of 20 mM imidazole in buffer B (+/+) (buffer B
547 with 5 mM $MgCl_2$ and 5 mM cellobiose) with 0.025% (w/v) DDM. The bound protein was eluted
548 with 200 mM imidazole in buffer B containing 0.025% (w/v) DDM.

549 Finally, we performed a pull-down assay using $BcsD_{StrepII}$, purified BcsC_TPR; crude BcsAB.
550 $BcsD_{StrepII}$ (0.2 mg) and $_{H6}BcsC_TPR_{H6}$ (0.2 mg) were mixed with crude BcsAB (7 mL of DDM
551 extract); NaCl stock solution (5 M) was added to a final concentration of 500 mM NaCl. After
552 incubation for 3 h at 4 °C, the sample solution was loaded to 0.1 mL of Streptactin Sepharose HP.
553 After washing with 1 mL of buffer B (+/+) containing 0.025% (w/v) DDM, the bound protein
554 was eluted with 4 mM *d*-desthiobiotin in buffer B (+/+) containing 0.025% (w/v) DDM.

555 Prey protein without bait protein was used as a negative control for the pull-down assay using
556 the same procedures. The eluted fraction was analyzed by SDS-PAGE, followed by WB as
557 described later.

558

559 **Western blotting (WB) analysis**

560 Rabbit polyclonal antibodies against BcsA, BcsB, BcsC, and BcsD proteins were generated
561 with the synthetic peptide corresponding to a part of the C-terminus of BcsA (18, 20, 21, 37), the
562 C-terminus of BcsB (this study), the C-terminus of BcsC (37), and the loop between the β3 and
563 β4-strand (20, 37). The dilution rate was 10,000-fold for anti-BcsA, anti-BcsB, and anti-BcsC,
564 whereas anti-BcsD was diluted 20,000-fold. Each of the antibodies against the peptide tag were
565 diluted as follows: anti-Strep tag II (15 ng/mL; ab180957, Abcam Corp., Cambridge, UK), anti-
566 His5 (0.1 μg/mL; 34660, Qiagen N.V., Germany), and anti-Thioredoxin (1 μg/mL; ab139677,
567 Abcam Corp.).

568 Horseradish peroxidase (HRP)-conjugated anti-rabbit IgG (W401B; Promega Inc.) and HRP-
569 conjugated anti-mouse IgG (7076S; Cell Signaling Technology Inc., MA, USA) were diluted
570 20,000-fold and used as the secondary antibodies. ECL-Prime (Cytiva Inc.) was used for
571 chemical luminescence with HRP.

572 For the WB with anti-BcsD, anti-Strep, anti-His, and anti-thioredoxin, the samples for SDS-
573 PAGE were heat-treated at 100°C for 3 min after mixing with the sample buffer, while the

574 samples to visualize by the other antibodies were incubated in the sample buffer for several
575 minutes at room temperature. The samples were analyzed by SDS-PAGE with a precast
576 polyacrylamide gel (SuperSep Ace 5-20%, Fujifim Wako Chemicals Co. Ltd.), and blotting from
577 the gel to PVDF membrane (Immobilon-P, 0.45 μm-ϕ, Cytiva Inc.) was done by a constant
578 current mode at 150 mA/10 cm^2 for 30 min. Blocking of the membrane was performed with 0.3%
579 skim milk and 0.02% NaN_3 in tris-buffered saline (TBS) containing 0.05% Tween-20 (TBS-T),
580 for the WB with anti-Bcs proteins, while blocking was performed with 2.5% BSA, 0.1% gelatin,
581 0.02% Tween-20, 0.04% NaN_3 in PBS at 4°C overnight or at room temperature for 0.5–1 h, for
582 either of anti-Strep-tag II, anti-His5, or anti-thioredoxin. The membranes were briefly rinsed with
583 TBS-T and then subjected to the primary antibody reaction in blocking buffer for 1–2 h at room
584 temperature. After removing the antibody solution, the membrane was briefly rinsed and washed
585 with TBS-T thrice for 5 min, followed by a secondary antibody reaction in TBS-T for 30–45 min
586 at room temperature. The membrane was briefly rinsed and washed with TBS-T three times for
587 15 min each time. The protein bands were then visualized by casting the ECL prime solution on
588 the blotted PVDF membrane (0.2 mL/9 cm^2 membrane), and digitally recorded with AE-9300H
589 EZ-Capture MG (ATTO Co. Ltd., Japan).

590 Quantitative analysis was performed using ImageJ (version 1.53a) to quantify the band signal
591 intensity, calculated as relative values to the negative control, and the relative signal intensities of
592 BcsA and BcsB were normalized to the signal intensity of BcsD. For BcsA; two major bands
593 were reproducibly observed near the 75-kDa and 250-kDa marker (Fig. 2B, top row), as well as
594 in our previous studies (18, 37), which are probably BcsA monomer and BcsA-including
595 oligomer, respectively (the estimated molecular weight for the BcsA monomer is 84 kDa). Given
596 these observations, the band intensity for the BcsA-containing oligomer was also considered in
597 addition to the monomer band intensity in subsequent analyses.

598
599
600 **Acknowledgments**
601
602 The authors thank Dr. Kenji Tajima of Hokkaido University for his advice. The authors thank
603 Professor Ryoichi Yamaji and Dr. Yasuyuki Kobayashi at Osaka Prefecture University for their
604 advice regarding the pull-down assay. This work was supported by JPSP KAKENHI (grant
605 numbers 15H04530 and 19H00950 to T. I.) and Exploratory Research on Humanosphere Science
606 (RISH, Kyoto University). We would like to thank Prof. Junji Sugiyama for JST CREST (grant
607 number: JPMJCR13B2).

608
609
610 **References**

611 1. J. L. W. Morgan, J. Strumillo, J. Zimmer, Crystallographic snapshot of cellulose synthesis
612 and membrane translocation. *Nature* **493**, 181-186 (2013).
613 2. J. L. W. Morgan, J. T. McNamara, J. Zimmer, Mechanism of activation of bacterial
614 cellulose synthase by cyclic di-GMP. *Nat. Struct. Mol. Biol.* **21**, 489-496 (2014).
615 3. U. Römling, M. Y. Galperin, Bacterial cellulose biosynthesis: Diversity of operons,
616 subunits, products, and functions. *Trends Microbiol.* **23**, 545-557 (2015).
617 4. W. Thongsomboon *et al.*, Phosphoethanolamine cellulose: A naturally produced
618 chemically modified cellulose. *Science* **359**, 334-338 (2018).
619 5. K. Tajima, T. Imai, T. Yui, M. Yao, I. Saxena, Cellulose-synthesizing machinery in bacteria.
620 *Cellulose* (2021). https://doi.org/10.1007/s10570-021-04225-7

621 6. H. C. Wong *et al.*, Genetic organization of the cellulose synthase operon in Acetobacter
622 xylinum. *Proc. Natl. Acad. Sci.U.S.A.* **87**, 8130-8134 (1990).
623 7. I. M. Saxena, K. Kudlicka, K. Okuda, R. M. Brown Jr, Characterization of genes in the
624 cellulose-synthesizing operon (acs operon) of Acetobacter xylinum: Implications for
625 cellulose crystallization. *J. Bacteriol.* **176**, 5735-5752 (1994).
626 8. R. Standal *et al.*, A new gene required for cellulose production and a gene encoding
627 cellulolytic activity in Acetobacter xylinum are colocalized with the bcs operon. *J.*
628 *Bacteriol.* **176**, 665-672 (1994).
629 9. S. Kawano *et al.*, Effects of endogenous endo-β-1,4-glucanase on cellulose biosynthesis in
630 Acetobacter xylinum ATCC23769. *J. Biosci. Bioeng.* **94**, 275-281 (2002).
631 10. K. Tajima *et al.*, Cloning and sequencing of the beta-glucosidase gene from *Acetobacter*
632 *xylinum* ATCC 23769. *DNA Res.* **8**, 263-269 (2001).
633 11. N. Tonouchi *et al.*, A beta-glucosidase gene downstream of the cellulose synthase operon
634 in cellulose-producing acetobacter. *Biosci. Biotechnol. Biochem.* **61**, 1789-1790 (1997).
635 12. J. T. McNamara, J. L. W. Morgan, J. Zimmer (2015) A molecular description of cellulose
636 biosynthesis. in *Annu. Rev. Biochem.* (Annual Reviews Inc.), pp 895-921.
637 13. A. Kumagai *et al.*, Ultrafine Cellulose Fibers Produced by Asaia bogorensis, an Acetic Acid
638 Bacterium. *Biomacromolecules* **12**, 2815-2821 (2011).
639 14. P. A. Penttilä *et al.*, Multimethod approach to understand the assembly of cellulose fibrils
640 in the biosynthesis of bacterial cellulose. *Cellulose* (2018).
641 15. S. Q. Hu *et al.*, Structure of bacterial cellulose synthase subunit D octamer with four inner
642 passageways. *Proc. Natl. Acad. Sci.U.S.A.* **107**, 17957-17961 (2010).
643 16. N. Sunagawa *et al.*, Cellulose complementing factor (Ccp) is a new member of the cellulose
644 synthase complex (terminal complex) in *Acetobacter xylinum*. *J. Biosci. Bioeng.* **115**, 607-
645 612 (2013).
646 17. O. Omadjela *et al.*, BcsA and BcsB form the catalytically active core of bacterial cellulose
647 synthase sufficient for in vitro cellulose synthesis. *Proc. Natl. Acad. Sci.U.S.A.* **110**, 17856-
648 17861 (2013).
649 18. T. Imai, S.-j. Sun, Y. Horikawa, M. Wada, J. Sugiyama, Functional reconstitution of
650 cellulose synthase in *Escherichia coli*. *Biomacromolecules* **15**, 4206–4213 (2014).
651 19. J. Du, V. Vepachedu, S. H. Cho, M. Kumar, B. T. Nixon, Structure of the cellulose synthase
652 complex of *Gluconacetobacter hansenii* at 23.4 Å resolution. *PLoS ONE* **11**, e0155886
653 (2016).
654 20. S.-j. Sun, T. Imai, J. Sugiyama, S. Kimura, CesA protein is included in the terminal
655 complex of Acetobacter. *Cellulose* **24**, 2017–2027 (2017).
656 21. S.-j. Sun, Y. Horikawa, M. Wada, J. Sugiyama, T. Imai, Site-directed mutagenesis of
657 bacterial cellulose synthase highlights sulfur–arene interaction as key to catalysis.
658 *Carbohydr. Res.* **434**, 99–106 (2016).
659 22. J. F. Acheson, R. Y. Ho, N. F. Goularte, L. Cegelski, J. Zimmer, Molecular organization of
660 the E. coli cellulose synthase macrocomplex. *Nat. Struct. Mol. Biol.* **28**, 310-318 (2021).
661 23. C. R. Santos *et al.*, Dissecting structure-function-stability relationships of a thermostable
662 GH5-CBM3 cellulase from *Bacillus subtilis* 168. *Biochem. Journal* **441**, 95-104 (2012).
663 24. J. F. Acheson, Z. S. Derewenda, J. Zimmer, Architecture of the Cellulose Synthase Outer
664 Membrane Channel and Its Association with the Periplasmic TPR Domain. *Structure* **27**,
665 1855-1861 (2019).
666 25. S. Nojima *et al.*, Crystal structure of the flexible tandem repeat domain of bacterial
667 cellulose synthesis subunit. *Sci. Rep.* **7**, 13018 (2017). https://doi.org/10.1038/s41598-017-
668 12530-0
669 26. A. Perez-Riba, L. S. Itzhaki, The tetratricopeptide-repeat motif is a versatile platform that

670 enables diverse modes of molecular recognition. *Curr. Opin. Struct. Biol.* **54**, 43-49 (2019).
671 27. W. Abidi, S. Zouhir, M. Caleechurn, S. Roche, P. V. Krasteva, Architecture and regulation
672 of an enterobacterial cellulose secretion system. *Sci. Adv.* **7**, eabd8049 (2021).
673 28. T. Uto *et al.*, Molecular Dynamics Simulation of Cellulose Synthase Subunit D Octamer
674 with Cellulose Chains from Acetic Acid Bacteria: Insight into Dynamic Behaviors and
675 Thermodynamics on Substrate Recognition. *J.Chem. Theory Comput.* **17**, 488-496 (2021).
676 29. H. Toyosaki *et al.*, Screening of Bacterial Cellulose-producing Acetobacter Strains Suitable
677 for Agitated Culture. *Biosci. Biotechnol. Biochem.* **59**, 1498-1502 (1995).
678 30. T. Nakai *et al.*, Control of expression by the cellulose synthase (*bcsA*) promoter region
679 from *Acetobacter xylinum* BPR 2001. *Gene* **213**, 93-100 (1998).
680 31. F. Rao *et al.*, Enzymatic synthesis of c-di-GMP using a thermophilic diguanylate cyclase.
681 *Analytical Biochemistry* **389**, 138-142 (2009).
682 32. A. Crameri, E. A. Whitehorn, E. Tate, W. P. C. Stemmer, Improved green fluorescent
683 protein by molecular evolution using DNA shuffling. *Nat. Biotechnol.* **14**, 315-319 (1996).
684 33. https://www.gene.mie-u.ac.jp/Protocol/Original/Transform-Comp-Cell-Freeze.html, the
685 latest access date: Mar 26 2022
686 34. D. M. Updegraff, Semimicro determination of cellulose inbiological materials. *Anal.*
687 *Biochem.* **32**, 420-424 (1969).
688 35. J. Stahlberg, G. Johansson, G. Pettersson, Trichoderma reesei has no true exo-cellulase: All
689 intact and truncated cellulase produce new reducing end groups on cellulose. *Biochim.*
690 *Biophys. Acta Gen. Subj.* **1157**, 107-113 (1993).
691 36. F. W. Studier, Protein production by auto-induction in high density shaking cultures.
692 *Protein Expr. Purif.* **41**, 207-234 (2005).
693 37. A. Hashimoto *et al.*, Extraction of cellulose-synthesizing activity of *Gluconacetobacter*
694 *xylinus* by alkylmaltoside. *Carbohydr. Res.* **346**, 2760–2768 (2011).
695
696

697 **Figures and Tables**

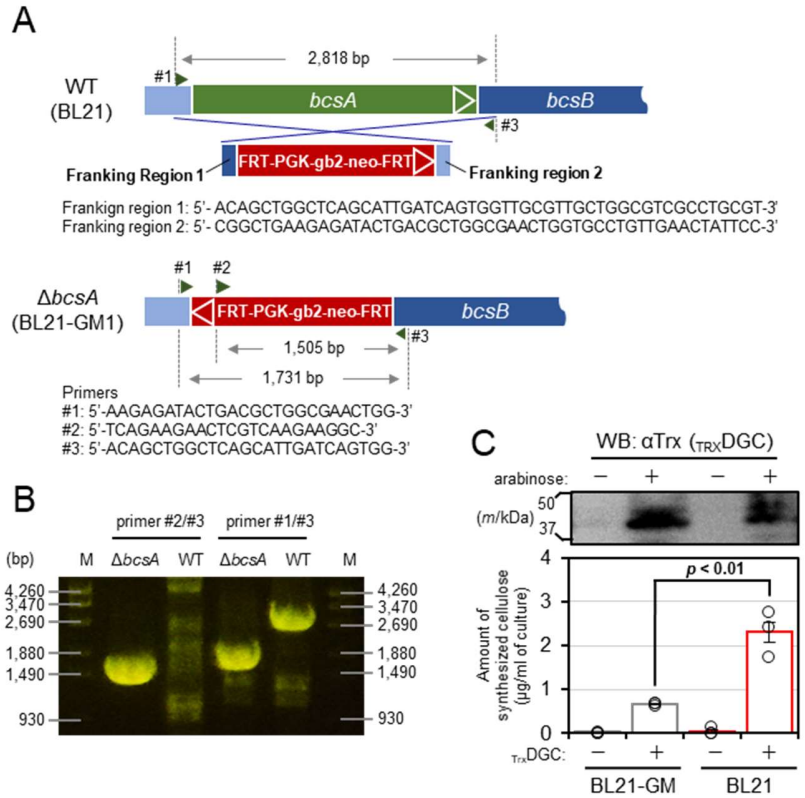

698
699

700 **Figure 1. Deletion of the *E. coli* endogenous *bcsA* gene**

701 **A** Schematic diagram of the experiment for deleting the endogenous *bcsA* gene using the Red/ET
702 recombination system. The primer sequences used are listed in Table S1. **B** Electrophoresis
703 pattern of colony-direct PCR using two pairs of primers. M: Molecular weight marker (Marker 6
704 (Nippon Gene Co. Ltd., Tokyo, Japan)); Δ*bcsA*: *bcsA*-deleted BL21; WT: wild-type BL21. **C**
705 Quantification of endogenous cellulose synthesis in BL21-GM and BL21 cells. The CESEC
706 system (18), which uses DGC expression to synthesize c-di-GMP to activate bacterial cellulose
707 synthase, was used to count the amount of cellulose that used DGC expression (bottom). The
708 expression of DGC was confirmed by WB using an anti-Trx antibody (top). The experiments
709 were performed in triplicate ($n = 3$) and are represented as mean ± standard error of the mean
710 (SEM), together with each of the data values. Statistical tests (Student's t-test) were performed
711 using the built-in function in Microsoft Excel (TTEST).

712

713

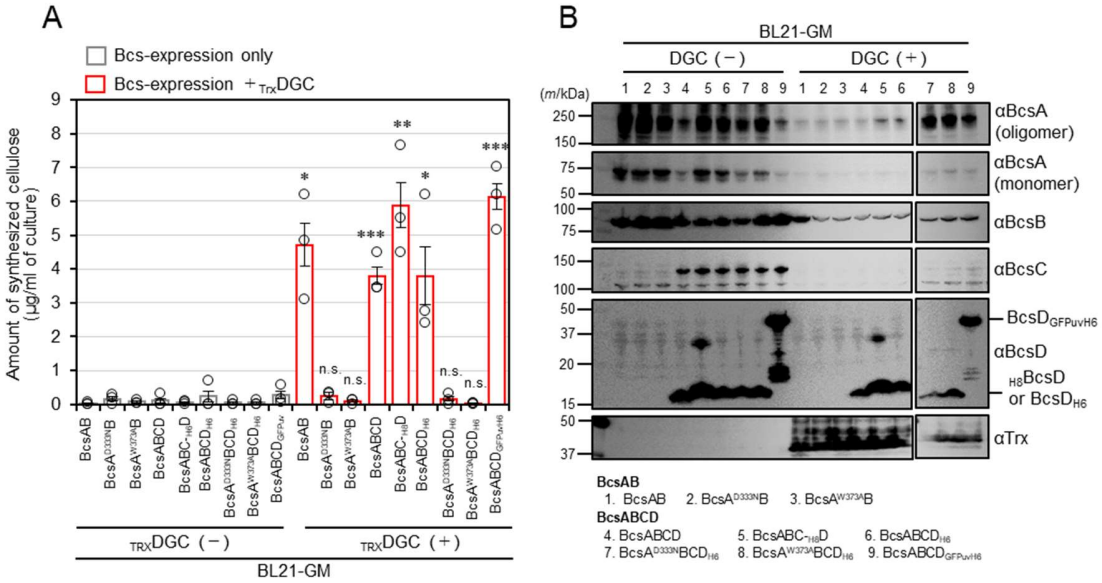

Figure 2. *in vivo* cellulose-synthesizing activity of recombinant Bcs-complex

A Cellulose-synthesizing activity of the recombinant Bcs-complexes tested in this study: the amount of cellulose synthesized by the CESEC system (18) with BL21-GM (Δ*bcsA*) is shown for each recombinant protein. All experiments were performed in triplicate ($n = 3$) and are represented as mean ± SEM together with the significance of difference: * for $p < 0.05$, ** for $p < 0.01$, *** for $p < 0.001$, and *n.s.* for not significant ($p > 0.1$) as a result of Student's t-test, which was performed using the built-in function of Microsoft Excel (TTEST). **B** Western blotting (WB) was performed for the CESEC experiment to check the expression of BcsA, BcsB, BcsC, BcsD, and TRXDGC. Cultures with and without DGC expression were tested. For BcsA, the data are shown separately for the oligomer and monomer bands. Due to the limited number of wells in the SDS-PAGE gel, the gel was divided into two parts for electrophoresis.

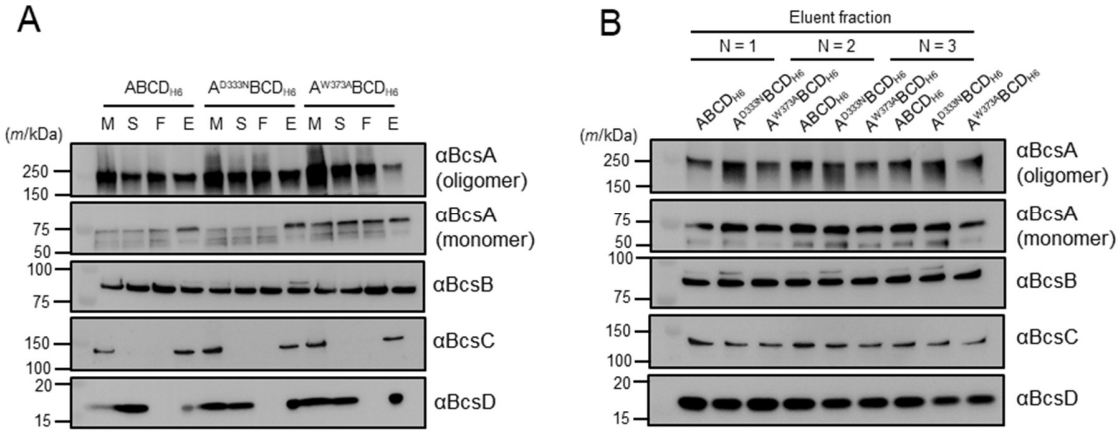

Figure 3. Purification of BcsABCD$_{H6}$

A Western blotting (WB) analysis of the purification process: M, membrane fraction; S, solubilized fraction; F, IMAC unbound fraction; E, IMAC-eluted fraction. Three protein samples, wild-type (BcsABCD$_{H6}$), D333N on BcsA (BcsA^{D333N}BCD$_{H6}$), and W373A on BcsA (BcsA^{W373A}BCD$_{H6}$), were analyzed using the antibodies indicated. **B** WB analyses of the eluate from three independent purification experiments for each of the three protein samples.

Approximately 2 µg of the protein was loaded onto the gel for WB with BcsA, BcsB, and BcsC antibodies, and 1 µg of the protein was added to the gel for WB with BcsD antibody. For BcsA, the data are shown separately for the oligomer and monomer bands.

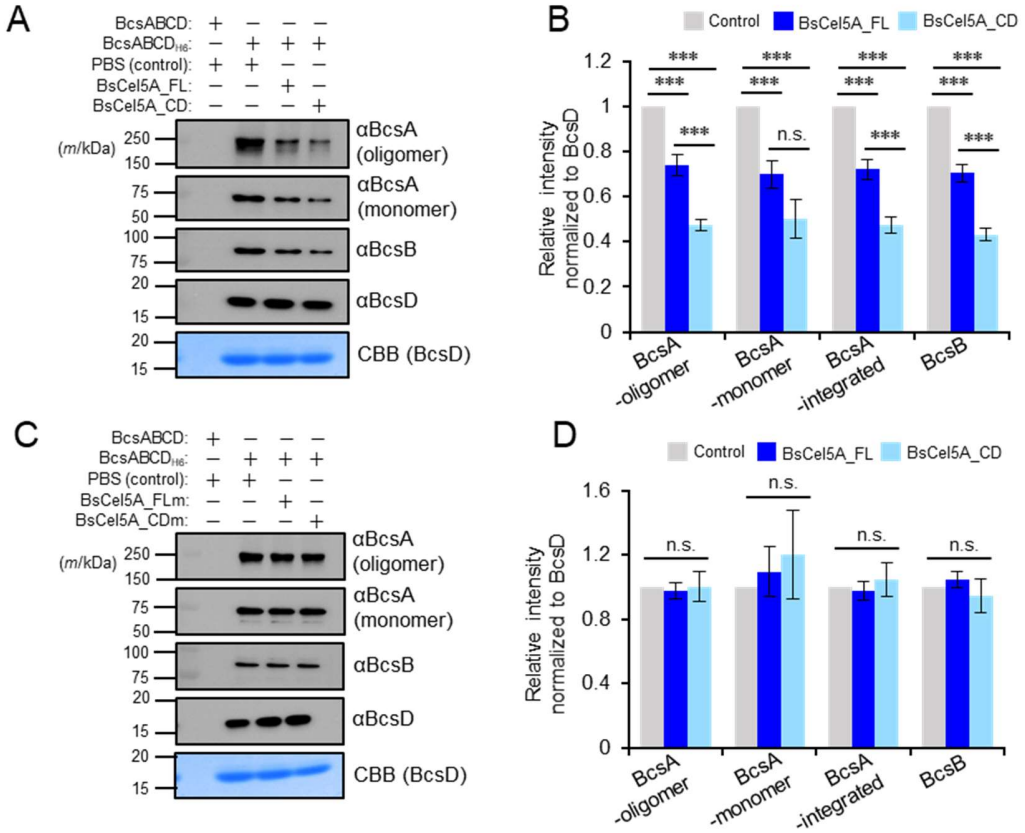

Figure 4. Effect of cellulase treatment to the purification of Bcs-complex

A, Western blot images of IMAC-eluted fractions of BcsWTBCD$_{H6}$ after treatment with wild-type cellulase (BsCel5A_FL and BsCel5A_CD). Coomassie Brilliant Blue (CBB)-stained images were used as loading controls. **B** Band intensity in western blot analysis of **A**. Error bars indicate standard error (SE), and the significance of the difference as a result of Student's *t*-test, which was performed using the built-in function of Microsoft Excel (TTEST), is indicated by the symbols: ** for $p < 0.01$, *** for $p < 0.001$, and *n.s.* for not significant ($p > 0.1$). **C**, Western blot images of IMAC-eluted fractions of BcsWTBCD$_{H6}$ after cellulase mutant (BsCel5A_FLm and BsCel5A_CDm) treatment. CBB-stained images were visualized using BcsD as a loading control. **D**, Band intensity in western blot analysis of **C**. Error bars indicate SEM, and Student's *t*-test, which was performed using the built-in function of Microsoft Excel (TTEST), showed no significant difference ($p > 0.1$; eight independent replicates).

For BcsA, the data are shown separately for the oligomer band, monomer band, and their sum. Each elution sample (~0.2 mg/mL) was added to an SDS-PAGE gel in 10 µL (anti-BcsA and anti-BcsB) and 1 µL (anti-BcsD and CBB stain), respectively. Elution samples for CBB staining were loaded into gel wells 10-fold more than those for WB (BcsD lane).

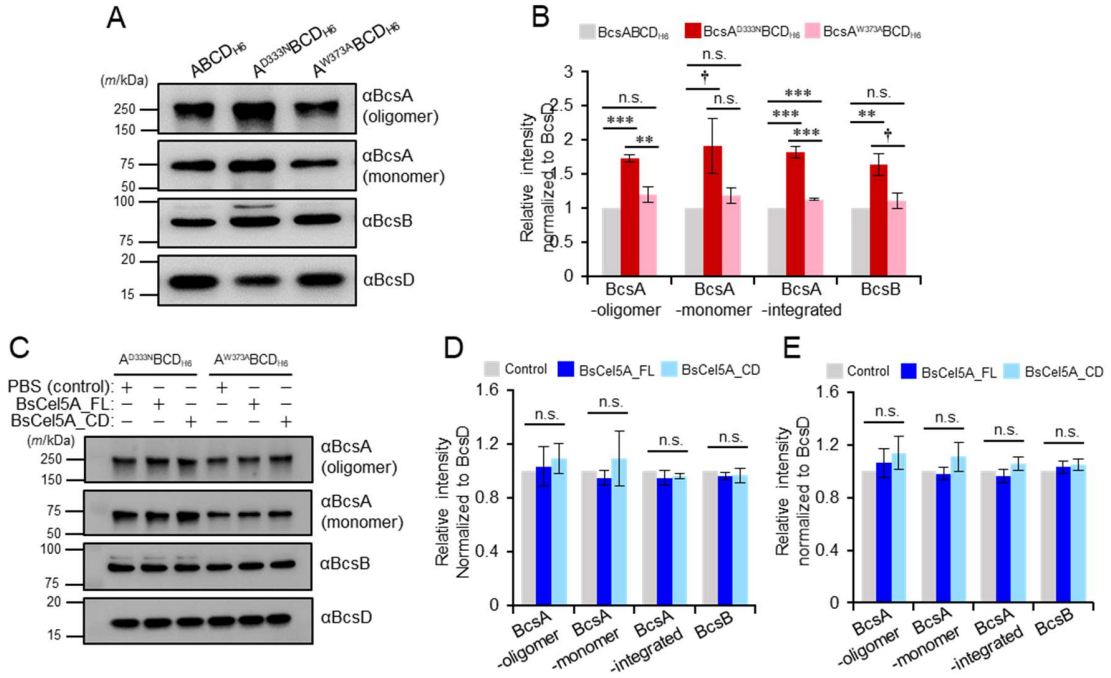

Figure 5. Effect of cellulase treatment on the purification of mutant Bcs-complex

A Western blot images of IMAC-eluted fractions of BcsWTBCD$_{H6}$, BcsA^{D333N}BCD$_{H6}$, and BcsA^{W373A}BCD$_{H6}$. CBB-stained images were visualized using BcsD as a loading control. **B** Band intensity in western blot analysis of **A**. An error bar indicates SEM, and the significance of the difference as a result of Student's *t*-test, which was performed using the built-in function of Microsoft Excel (TTEST), is indicated by the symbols † for $p < 0.1$, ** for $p < 0.01$, *** for $p < 0.001$, and *n.s.* for not significant ($p > 0.1$). **C**, Western blot images of IMAC-eluted fractions of BcsA^{D333N}BCD$_{H6}$ and BcsA^{W373A}BCD$_{H6}$ after treatment with wild-type cellulase (BsCel5A_FL and BsCel5A_CD). **D** and **E** Band intensity on western blot analysis of **C**: D for BcsA^{D333N}BCD and E for BcsA^{W373A}BCD. An error bar indicates SEM, and the significance of the difference as a result of Student's *t*-test, which was performed using the built-in function of Microsoft Excel (TTEST), showed no significant difference between any dataset.

All experiments were performed with four independent replicates ($n = 4$). For BcsA, the data are shown separately for the oligomer band, monomer band, and their sum. Each elution sample (~0.2 mg/mL) was added to an SDS-PAGE gel in 10 µL (anti-BcsA and anti-BcsB) and 1 µL (anti-BcsD and CBB stain), respectively. Elution samples for CBB staining were loaded into gel wells 10-fold more than those for WB (BcsD lane).

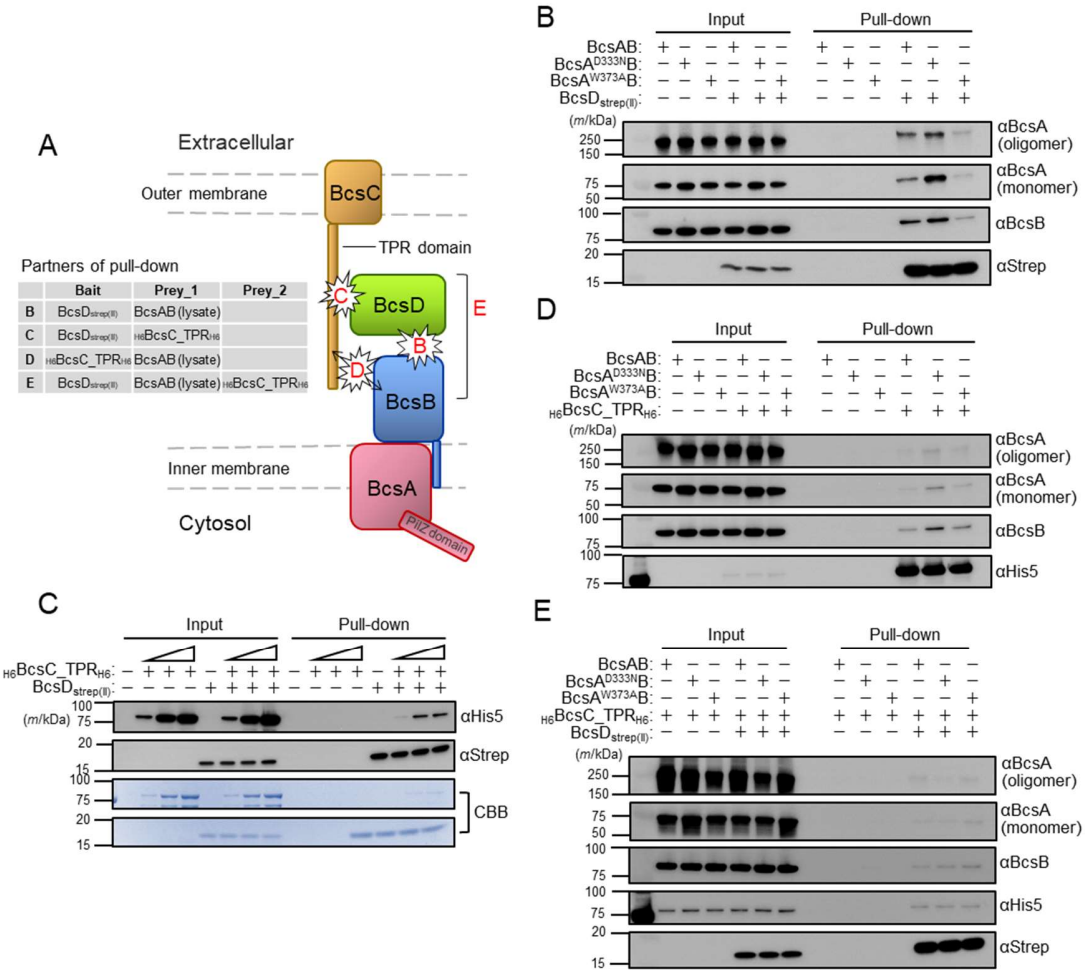

Figure 6. Pull-down assay with the Bcs subunits

A Schematic diagram showing the partners (bait and prey proteins) in a pull-down assay for each subunit of BcsABCD. Alphabets on the cartoon indicate panels B–D (the result of pull-down experiments), by which the subunit-subunit interaction was surveyed. **B** Western blot images of the pull-down assay using $BcsD_{StrepII}$ (bait) with crude BcsAB (prey). The pull-down fraction was analyzed by western blot using anti-BcsA, anti-BcsB, and anti-Streptag antibodies. **C** Western blot images of the pull-down assay using $BcsD_{StrepII}$ (bait) with purified $_{H6}BcsC_TPR_{H6}$ (prey). The pull-down fraction was analyzed by CBB staining and western blotting using anti-His5 and anti-Streptag antibodies. **D** Western blot images of the pull-down assay using $_{H6}BcsC_TPR_{H6}$ (bait) with crude BcsAB (prey). The pull-down fraction was analyzed by western blot using anti-BcsA, anti-BcsB, and anti-His5 antibodies. **E** Western blot images of the pull-down assay using $BcsD_{StrepII}$ (bait) with crude BcsAB (prey_1) and purified $_{H6}BcsC_TPR_{H6}$ (prey_2). The pull-down fraction was analyzed by western blot using anti-BcsA, anti-BcsB, anti-His5, and anti-Streptag antibodies. Input: sample immediately after mixing; pull-down: elution fraction after pull-down. All the detailed methods are described in the "Experimental Procedures" section of the text.

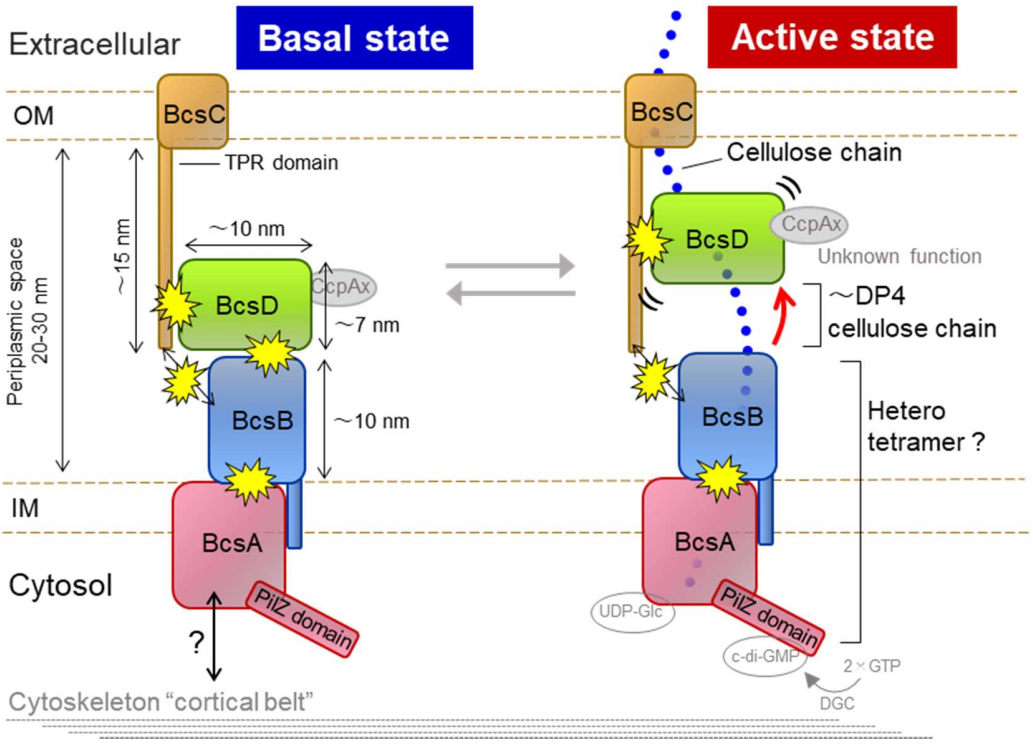

Figure 7. The hypothetical two-state model for the type I Bcs-complex

Hypothetical two-state model for the Bcs-complex: basal state (left) and active state (right). In this model, BcsD plays a key role in the periplasmic space to control the state of the complex separately from the state of the BcsA enzyme (1, 2). In the active state (right), BcsD draws the glucan chains in its octameric ring and brings those chains to the channel pore of BcsC in the outer membrane like a "button whirligig'. The TPR domain in BcsC may escort the BcsD protein to correctly transfer the glucan chains in BcsD to the BcsC channel. In the basal state (left), BcsD docks with the BcsB complex given that BcsB is located in the periplasmic space (1) as well as BcsD (12, 20). In the model, BcsD in the basal state also docks with BcsC without interfering with BcsB and is ready to draw the glucan chains in it once BcsAB starts synthesizing and extruding out the glucan chain. Thus, BcsD in this state may be a standby state for effectively transferring glucan chains into the extracellular space through the BcsC channel once BcsA is activated. Subunits that were not assessed in this study are indicated in gray.

808 Table 1. Experimental resources to express the proteins in this study

809

Material	Source	Description	Reference
		Bacterial cellulose synthase	
pQE-BcsAB (GOI* was inserted between EcoRI and KpnI site in pQE-80L vector (Qiagen Inc.))	LC428282 (*Komagataeibacter sucrofermentans* JCM9730)	Expression vector for BcsAB protein without tags	Imai et al. 2014
pQE-BcsA^{D333N}B (GOI* was inserted between EcoRI and KpnI site in pQE-80L vector (Qiagen Inc.))	LC428282 (*Komagataeibacter sucrofermentans* JCM9730)	Expression vector for BcsAB protein with a catalytic-deficient point mutation of D333N, without tags	Sun et al., 2016
pQE-BcsA^{W373A}B (GOI* was inserted between EcoRI and KpnI site in pQE-80L vector (Qiagen Inc.))	LC428282 (*Komagataeibacter sucrofermentans* JCM9730)	Expression vector for BcsAB protein with a catalytic-deficient point mutation of W373A, without tags	Sun et al., 2016
pQE-BcsABCD (GOI was inserted between EcoRI and HindIII site in pQE-80L vector (Qiagen Inc.))	LC687564 (*Komagataeibacter sucrofermentans* JCM9730)	Expression vector for BcsABCD complex without tags	This study
pQE-BcsABCD$_{H6}$ (GOI was inserted between EcoRI and HindIII site in pQE-80L vector (Qiagen Inc.))	LC687564 (*Komagataeibacter sucrofermentans* JCM9730)	Expression vector for BcsABCD complex with hexahistidine-tag at the C-terminal of BcsD protein	This study
pQE-BcsABC$_{H6}$D (GOI was inserted between EcoRI and HindIII site in pQE-80L vector (Qiagen Inc.))	LC687564 (*Komagataeibacter sucrofermentans* JCM9730)	Expression vector for BcsABCD complex with hexahistidine-tag at the N-terminal of BcsD protein	This study
pQE-BcsABCD$_{GFPuvH6}$ (GOI was inserted between EcoRI and HindIII site in pQE-80L vector (Qiagen Inc.))	LC687564 (*Komagataeibacter sucrofermentans* JCM9730)	Expression vector for BcsABCD complex with GFPuv followed by hexahistidine-tag at the C-terminal of BcsD protein	This study
pQE-BcsA^{D333N}BCD$_{H6}$ (GOI was inserted between EcoRI and HindIII site in	LC687564 (*Komagataeibacter*	Expression vector for BcsABCD complex with a catalytic-deficient point mutation of D333N	This study

pQE-80L vector (Qiagen Inc.))	*sucrofermentans* JCM9730)	introduced in BcsA; hexahistidine-tag is fused to the C-terminal of BcsD protein	
pQE-BcsA^{W373A}BCD$_{H6}$ (GOI was inserted between EcoRI and HindIII site in pQE-80L vector (Qiagen Inc.))	LC687564 (*Komagataeibacter sucrofermentans* JCM9730)	Expression vector for BcsABCD complex with a catalytic-deficient point mutation of W373A introduced in BcsA; hexahistidine-tag is fused to the C-terminal of BcsD protein	This study
pET-$_{H6}$BcsC_TPR$_{H6}$ (GOI was inserted between NdeI and XhoI site in pET28b (Novagene Inc.))	LC687564 (*Komagataeibacter sucrofermentans* JCM9730)	Expression vector for TPR domain of BcsC protein (Cys18 – Gly848): hexahistidine-tag is fused to both N- and C-terminal of the protein	This study
pET-BcsD$_{StrepII}$ (GOI was inserted between NcoI and HindIII site in pET28b vector (Novagen Inc.))	LC687564 (*Komagataeibacter sucrofermentans* JCM9730)	Expression vector for BcsD protein: Streptag(II) is fused to the C-terminal of BcsD protein	This study
Diguanylate cyclase (DGC)			
pBAD33et32-tDGC (Self-made vector in the previous study)	NP_229585 (*Thermotoga maritima* MSB8)	Expression vector of diguanylate cyclase with N-terminal truncation (K82 – S248) and a point mutation (R158A mutation): thioredoxin was fused to Nterminal end of the protein	This study
Cellulase			
pGEX-BsCel5A_FL (GOI was inserted between BamHI and XhoI site in pGEX4T-3 (GE Healthcare Inc.))	Z29076 (*Bacillus subtilis* strain 168)	Expression vector for full-length endoglucanase protein from *Bacillus subtilis* (BsCel5A): signal-peptide sequence (from Met1 to Ala28) was removed; GST-tag is fused to the N-terminal of BsCel5A protein, which consists of glycosylhydrolase 5 domain (GH-5 domain, Ala29 – Thr332) and carbohydrate-binding module (CBM-3, Ile354 – Asn499)	This study
pGEX-BsCel5A_CD (GOI was inserted between BamHI and XhoI site in pGEX4T-3 (GE Healthcare Inc.))	Z29076 (*Bacillus subtilis* strain 168)	Expression vector for catalytic domain (A29 – T332) of BsCel5A: GST-tag is fused to the N-terminal of the protein, which lacks the signal peptide sequence (Met1 – Ala28)	This study

pGEX-BsCel5A_FL^{m} (GOI was inserted between BamHI and XhoI site in pGEX4T-3 (GE Healthcare Inc.))	Z29076 (*Bacillus subtilis* strain 168)	Expression vector for full-length BsCel5A with activity-deficient double mutation (E169Q/E257Q): GST-tag is fused to the N-terminal of the protein, which lacks the signal peptide sequence (Met1 – Ala28)	This study
pGEX-BsCel5A_CD^{m} (GOI was inserted between BamHI and XhoI site in pGEX4T-3 (GE Healthcare Inc.))	Z29076 (*Bacillus subtilis* strain 168)	Expression vector for catalytic domain (A29 – T332) of BsCel5A with activity-deficient double mutation (E169Q/E257Q): GST-tag is fused to the N-terminal of the protein, which lacks the signal peptide sequence (Met1 – Ala28)	This study

* GOI: gene of interest